ISSN 1023-1935, Russian Journal of Electrochemistry, 2013, Vol. 49, No. 1, pp. 45–51. © Pleiades Publishing, Ltd., 2013.
Original Russian Text © N.A. Tarasova, Ya.V. Filinkova, I.E. Animitsa, 2013, published in Elektrokhimiya, 2013, Vol. 49, No. 1, pp. 50–56.

Electric Properties of Oxyfluorides $Ba_2In_2O_{5-0.5x}F_x$ with Brownmillerite Structure

N. A. Tarasova[z], Ya. V. Filinkova, and I. E. Animitsa

Ural Federal University Named after the First President of Russia B.N. Eltsin, ul. Mira 19, 620002 Ekaterinburg, Russia

Received July 13, 2011

Abstract—Synthesis of fluoro–substituted substances based on brownmillerite $Ba_2In_2O_5$ is carried out. The width of the homogeneity region of the $Ba_2In_2O_{5-0.5x}F_x$ ($0 < x \le 0.25$) solid solution was established using X-ray analysis. Measurement of temperature dependences of conductivity in atmospheres with different partial pressure of water vapor ($pH_2O = 3.3$ and 2×10^3 Pa) showed an increase in conductivity at $T \le 550$°C in a humid atmosphere, which is due to appearance of proton transport. The dependence of conductivity on partial oxygen pressure ($pO_2 = 0.21 \times 10^5$ to 10^{-15} Pa) is studied in the temperature range of 500–1000°C; ion transport numbers are calculated. The method of polarization measurements was used to determine transport numbers of fluoride. Total conductivity is divided into ion (proton, oxygen, and fluoride ion) and electron components. Analysis of concentration dependences of conductivities showed that low concentrations of fluoride allow increasing both the total and partial conductivities (oxygen–ion and proton) and, besides, allow shifting the "order–disorder" phase transition by 100°C to the low temperature range.

Keywords: brownmillerite, oxyfluoride, anion doping, ion conductivity

DOI: 10.1134/S102319351301014X

INTRODUCTION

Among the known high-temperature oxygen–ion and proton conductors with the structural disordering of the oxygen sublattice, barium indate $Ba_2In_2O_5$ stands out due to high nominal concentrations of oxygen vacancies and protons [1–9]. At the temperatures below 930°C, it is characterized by an orthorhombic brownmillerite structure, in which layers of oxygen octahedrons and tetrahedrons are alternated, as a result of which oxygen vacancies are ordered along the crystallographic direction [101]. However, at the temperatures above 930°C, an "order–disorder" phase transition occurs [7, 8]. Herewith, the structure is transformed from an orthorhombic one [9] to a defect perovskite structure with a statistical distribution of oxygen vacancies. This process is accompanied by a drastic increase in conductivity. In this connection, various methods of modification of this structure in order to enhance ion (oxygen or proton) conductivity are of interest.

Various methods of structure modification by substitution in the cation sublattice are described in the literature [10–20]. For example, donor doping results in a decrease in the concentration of oxygen vacancies, which promotes their statistical distribution in the structure and provides an increase in both the oxygen–ion and proton conductivity. One should point out that the main effect of cation doping is reduced to an increase in oxygen mobility and this, in its turn, leads to an increase in mobility of protons. In this connection, special interest is caused by direct exposure of the anion sublattice to doping, e.g., by introduction of F^- ions. One can assume that such substitution results in a decrease in the anion–hydrogen bond energy and increase in mobility of protons.

Analysis of phase equilibriums in the system of $BaO–BaF_2–In_2O_3$ shows the fundamental possibility of existence of fluoro-substituted phases on the basis of indium oxide, e.g., $Ba_3In_2O_5F_2$ [21] and Ba_2InO_3F [22]. Therefore, we performed partial substitution of oxygen ions by fluoride ions ($F^- \rightarrow O^{2-}$) in barium indate $Ba_2In_2O_5$.

As the concentration of fluoride ions can be changed in solid-phase synthesis by varying the BaO/BaF_2 ratio, one can assume in accordance with the quasichemical equation that introduction of fluoride ions results in a decrease in anion vacancies in the initial structure of $Ba_2In_2O_{5-0.5x}F_x[V_O]_{1-x}$:

$$\begin{aligned} &BaF_2 + V_O^x \rightarrow Ba_{Ba}^x + F_V' + F_O^\bullet, \\ &\rightarrow BaO \end{aligned} \qquad (1)$$

where V_O^x is the structural oxygen vacancy, Ba_{Ba}^x is the crystallographic position of barium, F_V' is fluoride in the anon vacancy site, $F_O^\bullet$ is fluoride in the oxygen site. Herewith, a decrease in the concentration of oxygen vacancies can promote stabilization of their statistical distribution and result in an increase in conductivity.

[z] Corresponding author: Natalia.Tarasova@usu.ru (N.A. Tarasova).

The aim of this work was to synthesize the $Ba_2In_2O_{5-0.5x}F_x$ solid solution, study its electrophysical properties and prove the occurrence of proton transport.

EXPERIMENTAL

Samples of $Ba_2In_2O_{5-0.5x}F_x$ ($0 \le x \le 2$) were obtained using the solid-phase synthesis technique from predehydrated $BaCO_3$, In_2O_3, BaF_2. Synthesis was carried out in air under a stepwise temperature increase (800–1200°C) and repeated grinding. A sample with $x = 0.00$ ($Ba_2In_2O_5$) was obtained and described earlier; here, it is synthesized for comparison.

X-ray analysis was carried out using a Bruker D8 Advance diffractometer in CuK_α radiation in the angle range of $2\theta = 10°–80°$. Lattice parameters were calculated using the Celref software.

Sample surface morphology, their cation composition and concentration distribution of elements were studied using a JEOL JSM 6390LA scanning electron microscope with an JEOL JED 2300 energy–dispersive add-on. The detection limit at usual energies (5–20 kV) was ~0.5 at %.

In order to measure electric properties, samples were prepared in the form of tablets; the sintering was carried out at the temperature of 1300°C for 24 h. The burning-in of platinum electrodes were carried out at the temperature of 900°C for 3 h.

Conductivity of the studied phases was measured in the atmosphere of different humidity and also under variation of pO_2.

Humid atmosphere was obtained by air bubbling at the room temperature successively through distilled water and saturated potassium bromide KBr solution ($pH_2O = 2 \times 10^3$ Pa). Dry atmosphere was provided by gas circulation through powdered phosphorus oxide P_2O_5 ($pH_2O = 3.3$ Pa). Besides, preliminary removal of carbon dioxide CO_2 from air was carried out to prevent the possible carbonization of ceramics: using a 20% NaOH solution for a humid atmosphere, using the Askarite reagent for a dry atmosphere. Gas humidity was controlled using an IVG-1 MK-S meter of gas humidity.

Conductivity was studied using the method of electrochemical impedance in the frequency range of 1 Hz–1 MHz with the signal amplitude of 0.015 V using the IPI-3 meter of impedance parameters. All electrochemical measurements were carried out under the conditions of equilibrium with T, pH_2O, pO_2. Bulk resistance was calculated using the Zview software. Specific conductivity was calculated according to the following equation:

$$\sigma_{sp} = \frac{1}{R}\left(\frac{l}{S}\right), \quad (2)$$

where l is the sample thickness, cm; S is the cross–section surface area, cm^2; R is the sample bulk resistance, Ohm, calculated on the basis of the electrochemical impedance data.

Conductivity under pO_2 variation was studied in the range of partial oxygen pressures of 0.21×10^5 to 10^{-15} Pa. Oxygen pressure was set and controlled using an "oxygen pump" and oxygen partial pressure sensor made of stabilized solid electrolyte based on ZrO_2.

Measurement of fluoride transport numbers was carried out using the polarization technique. To this end, the studied substance was placed into the electrochemical cell between platinum electrodes reversible by oxygen and electrons and irreversible by fluoride. Constant voltage was applied to the cell and the dependence of current drop on time was measured. While current i_o is determined at the initial moment of time by movement of all carrier types, current of F^- ions through the cell is blocked with time and the established steady–state current i_∞ is determined by transport of the remaining carriers. Thus, the ratio of the difference in the initial and steady–state currents to the initial current under the conditions of the blocking of electrodes by fluoride ions yields the fraction of fluoride–ion conductivity component:

$$t_{F^-} = \frac{i_o - i_\infty}{i_o}. \quad (3)$$

Thermal analysis was carried out using a NETZSCH STA 409 PC device combined with a QMS 403C Aëolos quadrupole mass spectrometer (NETZSCH) allowing simultaneous TG and DSC measurements in the temperature range of 40–1200°C at the heating rate of 10°/min. Prior to measurements, samples underwent thermal treatment in a humid atmosphere ($pH_2O = 2 \times 10^3$ Pa) by slow cooling from 1000 to 200°C at the rate of 1°/min to obtain hydrated sample forms.

RESULTS AND DISCUSSION

The synthesized samples were studied using the method of X-ray powder diffraction. It was found that the $Ba_2In_2O_{5-0.5x}F_x$ compositions are single-phase in the range of $0 \le x \le 0.25$ and are characterized by a brownmillerite structure with a body-centered orthorhombic lattice. Lattice parameters for $Ba_2In_2O_5$ agree with those described above [9]: a = 1.6740 nm, b = 0.6094 nm, c = 0.5959 nm (space group *Ibm*2, orthorhombic modification). The dependence of lattice parameters on the fluoride concentration is shown in Fig. 1. On the basis of the obtained data, one can show that introduction of fluoride into the anion sublattice does not noticeably affect the crystal lattice cell parameters. This is probably due to close radii of oxygen and fluoride ions ($r_{O^{2-}} = 0.140$ nm, $r_{F^-} = 0.133$ nm) [23]. Samples of compositions with $0.50 \le x \le 2.0$ were not single-phase; their phase composition is showed in Table 1.

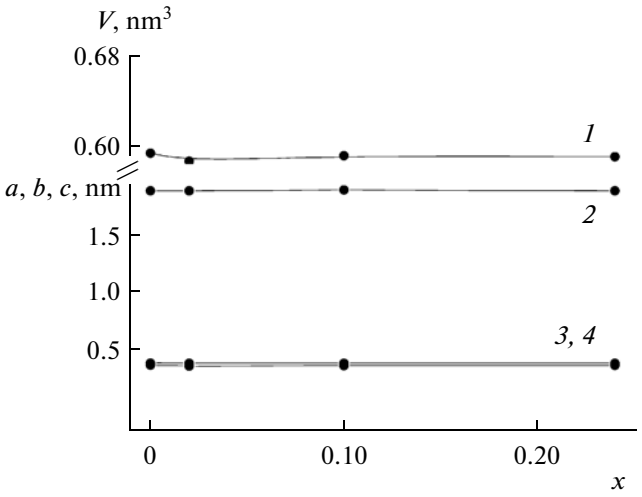

Fig. 1. Dependence of (*1*) cell volume and cell parameters ((*2*) *a;* (*3*, *4*) *b*, *c*) on the concentration of fluoride in $Ba_2In_2O_{5-0.5x}F_x$.

To confirm the cation composition of synthesized samples from the homogeneity region of the $Ba_2In_2O_{5-0.5x}F_x$ solid solution, studied were carried out using local X-ray energy–dispersive microanalysis. The data are presented in Table 2 at the example of the $Ba_2In_2O_{4.88}F_{0.25}$ formulation. One can see that good conservation of stoichiometry is observed; fluctuations of composition by metallic components did not exceed the measurement error.

Morphology of powder samples was studied using the method of scanning electron microscopy. Figure 2 shows the general view of the $Ba_2In_2O_{4.88}F_{0.25}$ sample surface in secondary electrons. One can see that the sample contains of large round grains with the size of 5–10 μm; no impurity phases were observed grain boundaries are pure.

Studies of total conductivity were carried out for compositions of the homogeneity region in atmospheres of different humidity (Fig. 3). It is found that the order–disorder phase transition characteristic for pure $Ba_2In_2O_5$ is preserved for samples with a low fluoride content. However, if it occurs near 900°C for an undoped composition, the temperature of phase transition decreases to 830°C for F-substituted samples. For composition with $x = 0.25$, a diffuse phase transition occurs. This order–disorder phase transition is manifested in the form of an endo effect of a DSC signal, as shown in Fig. 4. One can see that the temperature of the effect for pure barium indate corresponds to 920°C and its is shifted to 830°C in the case of a fluoro–substituted sample with $x = 0.10$. Thus, one can state a good correlation of the temperatures of the DSC effect and conductivity.

Comparison of conductivity polytherms (Fig. 3) in atmospheres of different humidity shows that the conductivity values of all samples at the temperature below 550°C increase in a humid atmosphere as compared to a dry one as a result of water intercalation and appearance of proton conductivity.

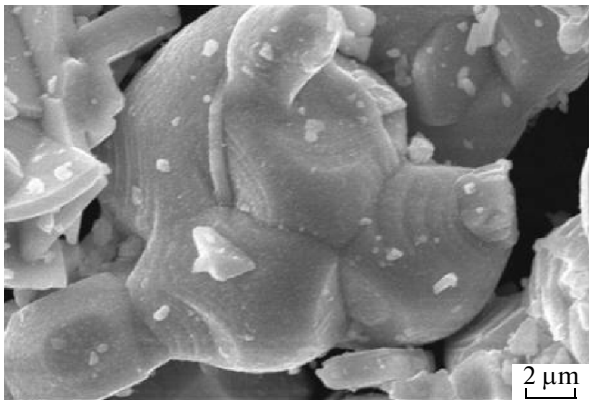

Fig. 2. SEM image of the surface of a $Ba_2In_2O_{4.88}F_{0.25}$ sample obtained in secondary electrons.

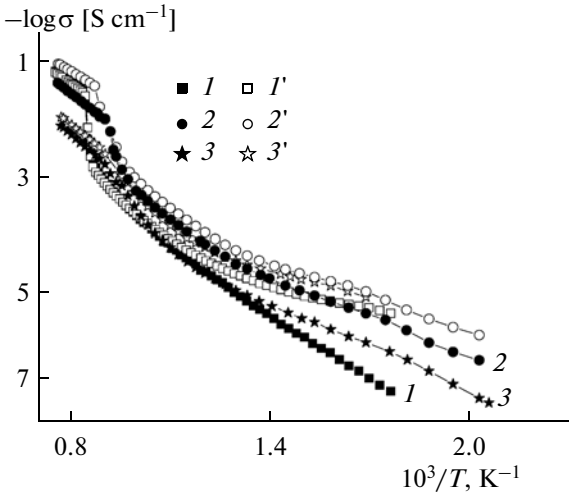

Fig. 3. Temperature dependence of conductivity for samples corresponding to the region of homogeneity of $Ba_2In_2O_{5-0.5x}F_x$ at *x*: (*1*, *1'*) 0, (*2*, *2'*) 0.02, (*3*, *3'*) 0.25 ((*1*–*3*) dry air, (*1'*–*3'*) humid air).

Figure 5 shows concentration dependences of total conductivity. One can see that the conductivity values pass through a maximum at $x = 0.02$ both in dry and in humid air.

Dependences of conductivity on oxygen partial pressure were studied for composition with $x = 0.10$ (Fig. 6). In a dry atmosphere, at the temperature

Table 1. Phase composition of $Ba_2In_2O_{5-0.5x}F_x$

x	Phase composition
0.5	$BaIn_2O_4$, $Ba_3In_2O_5F_2$, $Ba_2In_2O_{5-0.5x}F_x$
1.0	$BaIn_2O_4$, $Ba_3In_2O_5F_2$
1.5	$BaIn_2O_4$, $Ba_3In_2O_5F_2$, BaF_2
2.0	$BaIn_2O_4$, BaF_2

Table 2. Cation composition of a $Ba_2In_2O_{4.88}F_{0.25}$ sample according to the data of X-ray energy–dispersive microanalysis

No.	In, at %	Ba, at %	No.	In, at %	Ba, at %
1	49.50	50.50	15	50.99	49.01
2	50.95	49.05	16	50.98	49.02
3	50.91	49.09	17	50.99	49.01
4	51.60	48.40	18	50.65	49.35
5	51.63	48.37	19	51.10	48.90
6	51.05	48.95	20	51.19	48.81
7	51.18	48.82	21	50.42	49.58
8	50.51	49.49	22	50.79	49.21
9	50.48	49.52	23	49.84	50.16
10	50.60	49.40	24	50.21	49.79
11	51.10	48.90	25	50.81	49.19
12	50.64	49.36			
13	50.06	49.94	Average	**50.41**	**49.29**
14	50.40	49.60	Theoretical	**50.00**	**50.00**

below 700°C, the curves have a positive slope in the range of high pO_2 values; it is characterized by contribution of electron *p*-type conductivity. A plateau of pO_2 independence is observed in the range of medium and low pO_2 that points to ion conductivity. At the temperature above 750°C, conductivity is independent of the partial oxygen pressure in the whole studied range, which points to the predominant ion conductivity type in a wide range of pO_2. In a humid atmosphere, at low temperatures in the range of the "plateau", the total conductivity increases as compared to conductivity in a dry atmosphere by 0.7 order of magnitude, which results from an increase in the concentration of proton defects due to interaction with water vapors:

$$V_O^x + H_2O + 2O_O^x \Leftrightarrow 2OH_O^\bullet + O_i'', \quad (4)$$

where V_O^x is the structural oxygen vacancy, O_O^x is oxygen in a regular site, $OH_O^\bullet$ is a hydroxyl group in an oxygen site, O_i'' is oxygen in the structural vacancy site (technically, an interstice). Hole formation in the range of high pO_2 occurs according to the following quasichemical equation:

$$V_O^x + 1/2\,O_2 \leftrightarrow O_i'' + 2h^\bullet. \quad (5)$$

In a humid atmosphere, under interaction with water vapors, the hole concentration decreases and proton defects appear, which is described by the following equation:

$$h^\bullet + 1/2\,H_2O + O_O^x \Leftrightarrow 1/4\,O_2 + (OH)_O^\bullet. \quad (6)$$

On the basis of the fact that the range of conductivity independence of pO_2 reflects the ion character of conductivity, the total conductivity in calculations of partial contributions of conductivities in a wide range of pO_2 was approximated by an equation of the following type (T = const):

$$\sigma_{total} = \sigma_{el} + \sigma_{ion} = Kp O_2^{1/4} + \sigma_{ion}, \quad (7)$$

where ion conductivity σ_{ion} is independent of pO_2 and electron *p*-type conductivity corresponds to the function of $KpO_2^{1/4}$.

Knowing the partial contributions of conductivities, one can calculate ion transport numbers according to the following formula:

$$t_{ion} = \sigma_{ion}/\sigma_{total}. \quad (8)$$

Their temperature dependences are shown in Fig. 7 for the formulation with $x = 0.10$. In the presence of dry air, ion transport numbers grow at an increase in temperature. In the case of humid air, ion transport

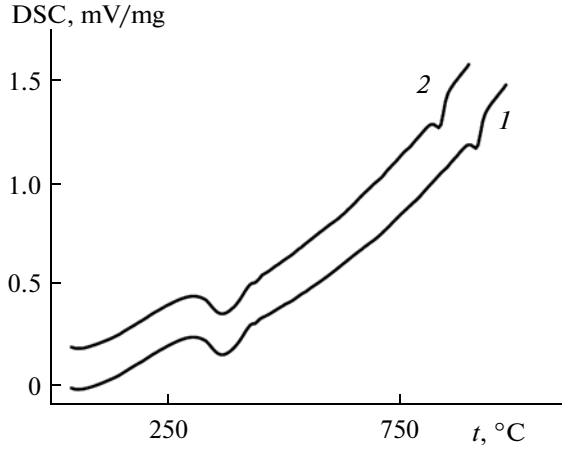

Fig. 4. Data of differential scanning calorimetry for the compositions of: (*1*) $Ba_2In_2O_5$, (*2*) $Ba_2In_2O_{4.95}F_{0.10}$.

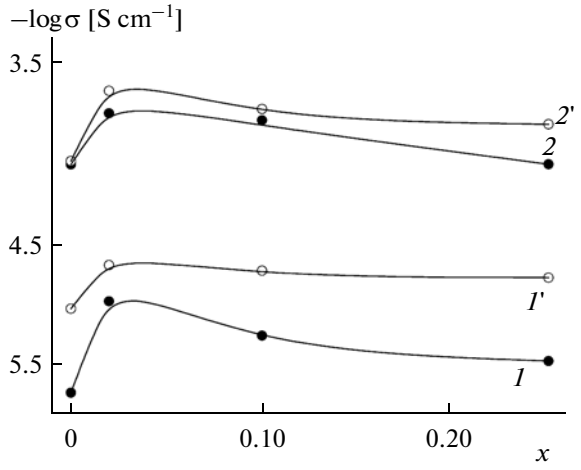

Fig. 5. Concentration dependences of conductivity for samples corresponding to the region of homogeneity of $Ba_2In_2O_{5-0.5x}F_x$ at different temperatures, °C: (*1*, *1'*) 400, (*2*, *2'*) 700 ((*1*, *2*) dry air, (*1'*, *2'*) humid air).

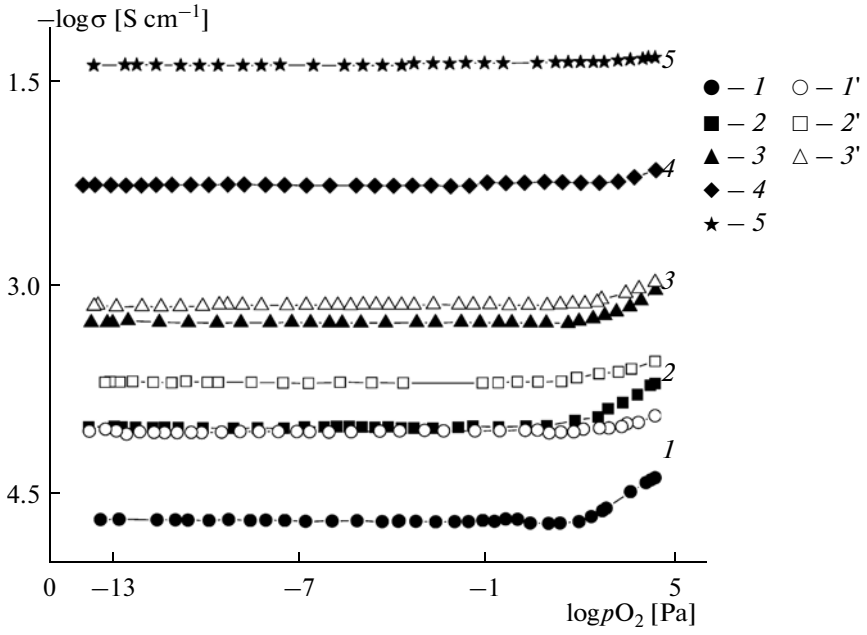

Fig. 6. Dependence of conductivity on the partial pressure of oxygen for the composition of $Ba_2In_2O_{4.95}F_{0.10}$ at different temperatures, °C: (*1*, *1'*) 500, (*2*, *2'*) 600, (*3*, *3'*) 700, (*4*) 825, (*5*) 900 ((*1*–*5*) dry air, (*1'*–*3'*) humid air).

numbers increase in the temperature range of 500–700°C as compared to those obtained in dry air as a result of appearance of the proton contribution. However, Σt_{ion} decreases at an increase in the temperature, as the fraction of proton transport decreases (water leaves the structure). The data of gravimetry and mass spectrometry confirm appearance of proton defects in the hydrated phase structure as a result of dissociative dissolution of water vapors in the oxide matrix (equation (4)). According to the TG data (Fig. 8), intensive mass loss in hydrated samples occurs in the temperature range of 300–400°C, which is accompanied by the presence of a small endo effect in the DSC curve (Fig. 4). Mass spectrometry analysis (Fig. 8) showed the presence of a peak with the mass number of 18, which clearly points to water evolution; no other volatile substances (including HF, CO_2) were found.

At a high temperature, water is completely removed from the sample, therefore the temperature dependences of Σt_{ion} for dry and humid air coincide at $T >$ 700°C (Fig. 7).

The transport numbers of fluoride calculated on the basis of polarization measurements for a dry atmosphere are shown in Fig. 7. One can see that they grow at an increase in the temperature and reach 55% at 1000°C. However, the fraction of F transport is low at the temperature below 600°C.

Pooling all data on transport numbers, one could construct concentration dependences of partial conductivities. Figure 9a shows the data for a dry atmosphere and high temperature, when the contribution of fluoride is noticeable and proton transport is negligible. The trend observed for the concentration dependence of the total conductivity is also manifested for partial conductivities (oxygen, fluoride–ion, and electron). The maximum values are observed for the $Ba_2In_2O_{4.99}F_{0.02}$ composition. The further increase in the fluoride concentration results in a decrease in partial conductivities. Figure 9b shows concentration dependences for a low temperature and in a humid atmosphere, when the contribution of the fluoride–

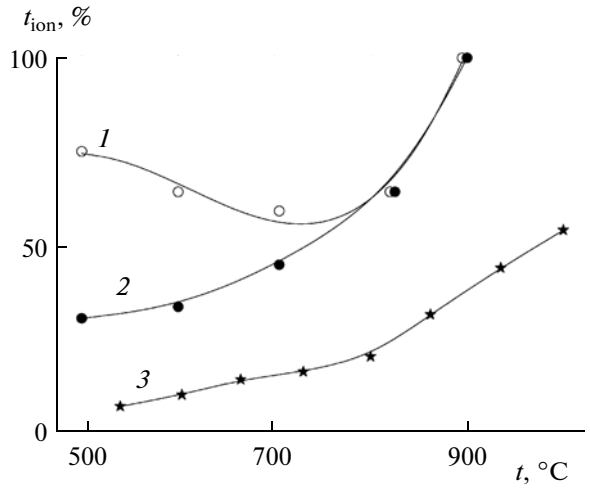

Fig. 7. Dependence of ion transport numbers on the temperature for the composition of $Ba_2In_2O_{4.95}F_{0.10}$ at $pO_2 = 0.21 \times 10^5$ Pa: (*1*) Σt_{ion} (humid air), (*2*) Σt_{ion} (dry air), (*3*) t_{F^-}.

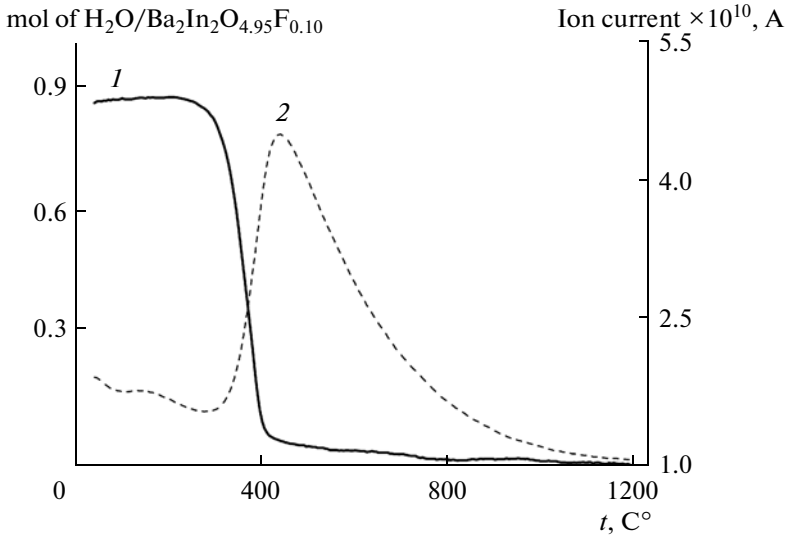

Fig. 8. Results of (*1*) thermogravimetric and (*2*) mass-spectrometer analysis of a hydrated $Ba_2In_2O_{4.95}F_{0.10}$ sample (the TG curve is given as per amount of mols of water).

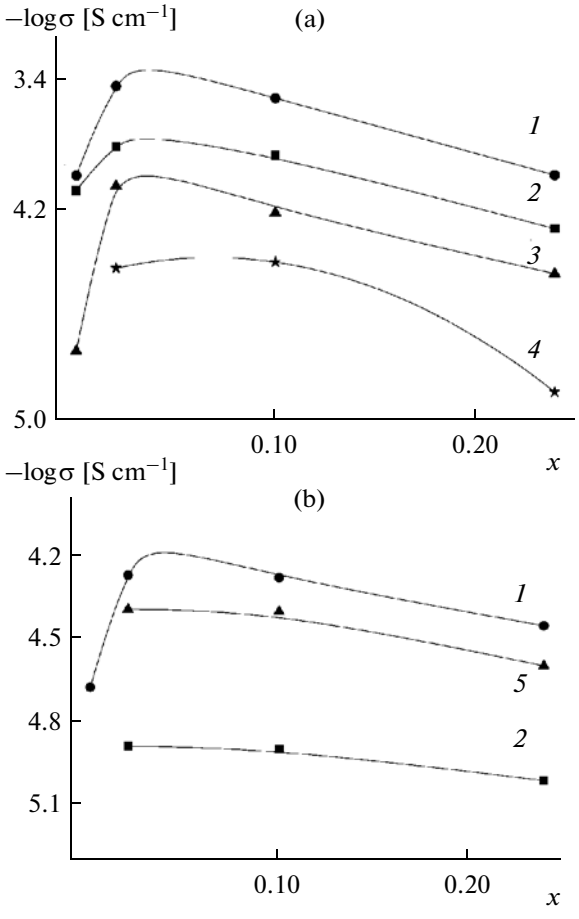

Fig. 9. Concentration dependences of partial conductivities: (*1*) σ_{total}, (*2*) σ_{el}, (*3*) $\sigma_{O^{2-}}$, (*4*) σ_{F^-}, (*5*) σ_{ion} for samples corresponding to the homogeneity region of $Ba_2In_2O_{5-0.5x}F_x$: (a) in dry air at 700°C, (b) in humid air at 500°C.

ion conductivity component is low and proton transport is considerable. Same as for a dry atmosphere, the maximum value of both the total and partial conductivities is characteristic of the formulation with $x = 0.02$. Ion conductivity becomes predominant under the conditions of a humid atmosphere at $T < 500$°C.

Thus, oxygen–deficient oxyfluorides $Ba_2In_2O_{5-0.5x}F_x$ ($0 \le x \le 0.25$) with a brownmillerite structure were synthesized for the first time. They are capable of dissociative water absorption from the gas phase and manifest proton transport. Conductivity is divided into components. It is shown that low fluoride concentrations allow increasing both the total and partial conductivity (O^{2-}, H^+) and allow shifting the order–disorder phase transition by 100°C towards lower temperatures.

ACKNOWLEDGMENTS

The work was financially supported by the Russian Foundation for Basic Research (project no. 12-03-31234 mol_a), Contest for Carrying out Research of Ural Federal University and Federal Target Program "Scientific and Scientific–Pedagogical Human Resources of Innovative Russia in 2009–2013."

REFERENCES

1. Prasanna, T.R. and Novrotsky, A., *J. Mater. Res.*, 1993, vol. 8, no. 7, p. 1484.
2. Norby, T., *Korean J. Ceram.*, 1998, vol. 2, no. 4, p. 128.
3. Schober, T. and Friedrich, J., *Solid State Ionics*, 1998, vol. 113-115, p. 369.
4. Fisher, C.A.J. and Islam, M.S., *Solid State Ionics*, 1999, vol. 118, p. 355.

5. Zhang, G.B. and Smyth, D.M., *Solid State Ionics*, 1995, vol. 82, p. 161.
6. Schober, T., Friedrich, J., and Krug, F., *Solid State Ionics*, 1997, vol. 99, p. 9.
7. Goodenough, J.B., Ruiz-Diaz, J.E., and Zhen, Y.S., *Solid State Ionics*, 1990, vol. 44, p. 21.
8. Zhang, G.B. and Smyth, D.M., *Solid State Ionics*, 1995, vol. 82, p. 153.
9. Fisher, W., Reck, G., and Schober, T., *Solid State Ionics*, 1999, vol. 116, p. 211.
10. Shimura, T. and Yogo, T., *Solid State Ionics*, 2004, vol. 175, p. 345.
11. Schober, T., *Solid State Ionics,* 1998, vol. 109, p. 1.
12. Murugaraj, P., Kreuer, K.D., He, T., Schober, T., and Maier, J., *Solid State Ionics*, 1997, vol. 98, p. 1.
13. Jayaraman, V., Magrez, A., Caldes, M., Jobert, O., Taulelle, F., Rodrigez-Carvajal, J., Piffard, Y., and Brohan, L., *Solid State Ionics*, 2004, vol. 170, p. 25.
14. Berastegui, P., Hull, S., Garcia-Garcia, F.J., and Eriksson, S.-G., *J. Solid State Chem.*, 2002, vol. 164, p. 119.
15. Hui, Rob., Maric, R., Deses-Petit, C., Styles, E., Qu, W., Zhang, X., Roller, J., Yick, S., Ghosh, D., Sakata, K., and Kenji, M., *J. Power Sources,* 2006, vol. 161, p. 40.
16. Rolle, A., Daviero-Manaud, S., Roussel, P., Rubbens, A., and Vannier, R.N., *Solid State Ionics*, 2008, vol. 179, p. 771.
17. Rolle, A., Vinnier, R.N., Giridharan, N.V., and Abraham, F., *Solid State Ionics,* 2005, vol. 176, p. 2095.
18. Ta, T.Q., Tsuji, T., and Yamamura, Y., *J. Alloys Compd.*, 2006, vol. 408–412, p. 253.
19. Yoshinaga, M., Yamaguchi, M., Furuya, T., Wang, S., and Hashimoto, T., *Solid State Ionics*, 2004, vol. 169, p. 9.
20. Mohn, C.E., Allan, N.L., and Stolen, S., *Solid State Ionics*, 2006, vol. 177, p. 223.
21. Needs, R.L. and Weller, M.T., *J. Chem. Soc., Dalton Trans.*, 1995, p. 3015.
22. Needs, R.L. and Weller, M.T., *J. Chem. Soc., Chem. Commun.*, 1995, vol. 3, p. 353.
23. Shannon, R.D., *Acta Cryst.*, 1976, vol. A32, p. 751.